A high resolution digital elevation model of the Greenland ice sheet and validation with airborne laser altimetry

Jonathan L Bamber | Centre for Remote Sensing, Dept of Geography, University Rd, Br BS8 1SS, UK

j.l.bamber bristol.ac.uk

http://www.ggy.bris.ac.uk/research/crs/crs.htm

Simon Ekholm | KMS (National Survey and Cadastre),Rentemestervej 8, DK-2400 Copenhagen NV Denmark

se kms.min.dk

William Krabill | NASA Goddard Space Flight Center, Wallops Flight Facility, Labora Hydrospheric Processes, Wallops Island, VA 233337, USA

krabill aol15.wff.nasa.gov

Abstract

A 2.5 km resloution digital elevation model (DEM) of the Greenland ice sheet has been produced from the full 336 days of the geodetic phase of ERS-1. During this period the altimeter was operating in ice-mode over land surfaces providing improved tracking around the margins of the ice sheet. Combining this with the high density of tracks during the geodetic phase results in a unique data set for deriving a high resolution DEM of the whole ice sheet. The errors present in the altimeter data, after data filtering, waveform retracking and slope induced error correction, have been investigated via a comparison with airborne laser altimeter measurements obtained for the southern half of Greenland during the period 1991-1993. The absolute accuracy of the airborne data was typically in the range 2-10 cm ± 10 cm. Comparison with the sattelite data at cross-overs showed a strong correlation with surface slope (as has been demonstrated before and would be expected). The bias between the two data sets ranged from 84 cm ± 79 cm for slopes below 0.1 degrees increasing to a bias of 10.3 m ± 8.4 m for a slope of 0.7 degrees (the half power beamwidth of the ERS-1 radar altimeter). An explanation for the behaviour of the bias as a function fo surface slope is given in terms of the pattern of surface roughness on the ice sheet.

Keywords: Greenland, topography, altimetry

Introduction

The geodetic phase of ERS-1 has provided unprecedented coverage of the whole of the Greenland ice sheet by radar altimetry. This is due to both the high density of tracks (4 km across track spacing at 60° latitude) and the use of the ice mode over land surfaces during this phase. The full 336 days of the geodetic phase data have been processed to produce a 2.5 km resolution digital elevation model (DEM) of the Greenland ice sheet. To validate the height measurements made by the radar altimeter (RA) a set of airborne laser altimeter flight-lines over southern Greenland were used (Figure 1).

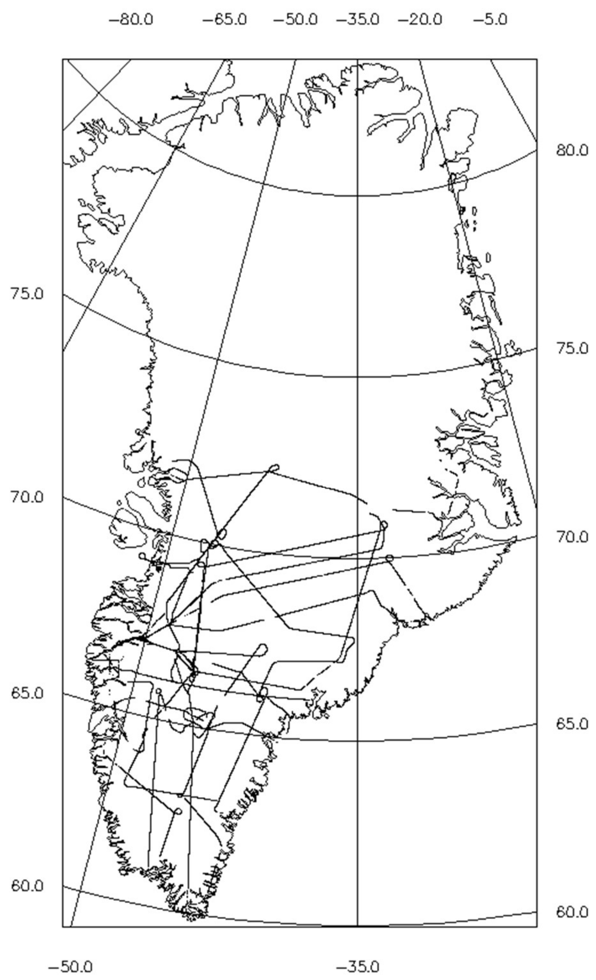

Figure 1. Plot of location of airborne laser altimeter flight lines used in as validation data.

These lines were flown between 1991 and 1993. The laser data have an absolute accuracy of » 10 cm with a standard deviation of 10-15 cm (Krabill *et al*, 1995) and provide, therefore, a benchmark for testing the reliability of the RA data (and the processing used on them). The methodology for processing the data and for making the comparison between the two data sets is described, briefly, in the next section. Section 3 presents the results of the comparison and section 4 is a discussion of the differences seen and likely explanations for these differences.

2. DATA REDUCTION & METHODOLOGY
2.1 Radar Data

The radar data reduction methodology has been described, in detail, elsewhere (Bamber, 1994; Bamber and Huybrechts, 1996) and only the most relevant points, therefore, are mentioned here. To improve the accuracy of elevation estimates over ice sheets it is necessary to apply a range estimate refinement procedure (known as waveform retracking) and a slope correction to provide the correct range and location for the corresponding sub-satellite ground point. The former was carried out using the offset centre of gravity method of calculating the wave-form amplitude, with a power threshold of 25%. This threshold was chosen as it best represents the mean height over a topographic surface (Partington, and others, 1989). Slope correction was applied using the relocation method with several modifications (Bamber, 1994). All the data were assimilated into a "slopes database" (in fact it is a range-rate database) which allows the reconstruction of the three-dimensional range-rate surface. This surface is then used to determine the actual location of the closest point to the satellite. The new position and range to this point is then calculated. This leads to a clustering of the points around the peak of an undulation and absence of points in the trough (Fig. 10, Bamber, 1994). This has important consequences for i) the methodology adopted for comparing the two data sets and ii) the introduction of biases in the radar data, discussed in subsequent sections.

Appropriate data filtering is required over non-ocean surfaces due to frequent occurrences of anomalous height returns. Fourteen different tests were applied to the return echo wave-form shape, backscatter coefficient, and retracking correction value for each altimeter height estimate. About 27 % of the data were removed during this filtering procedure. The majority of these bad data were associated with the altimeter having lost "lock" of the ice sheet surface, in areas of high relief, before the instrument software had registered that loss of lock had occurred. A further step was required to remove the occasional spurious orbit. These were identified by comparing one track with another at the point where they cross each other (known as cross-over analysis). The majority of poor orbits were found to be close, in time, to orbit manoeuvres of the satellite, even though the orbit manoeuvre flag in the data product was not set and had not been for one-two revolutions of the satellite.

Once the various corrections had been applied and filtering carried out, as described above, the data were interpolated onto a 2.5 km grid. A polar stereographic projection, with origin at the North Pole, and standard parallel of 71°S was used to translate from polar to Cartesian co-ordinates.

The spatial distribution of the altimeter data is highly anisotropic – height estimates are separated by 335 m along-track and by up to 4 km across-track. To prevent introducing biases on individual grid points (due to the spatial sampling pattern and grid spacing) a two-stage gridding procedure was employed. The first step involved producing local distance-weighted means of x, y and z in the region of a grid point, producing a quasi-regular array of average height estimates. A triangulation procedure was then used to interpolate to the exact grid point locations (Renka and Cline, 1984) and to extrapolate to grid points where no altimeter data were present. For validation purposes, however, the ungridded, individual radar data were used.

2.2 Laser Data

The laser altimeter data were collected by a scanning system known as the Airborne Oceanographic Lidar (AOL) which produced a series of concentric circles of approximately 200 m diameter. Thus a dense swath of points is obtained along a flight-line. A detailed description of the system characteristics has been presented elsewhere (Krabill *et al*, 1995) and only the most relevant points are described here. The laser spot diameter, on the surface, was about 1 m, in contrast to the pulse-limited footprint of the altimeter which can be as large as 20 km. The AOL data were supplied as an averaged value along the flight-line at about 25 m intervals. The standard deviation for each point (produced when averaging the "full swath" data) was also provided and proved useful for identifying occurrences of the laser "losing" the surface due to clouds, diamond dust or other atmospheric interference.

An example of an AOL profile is shown in Figure 2.

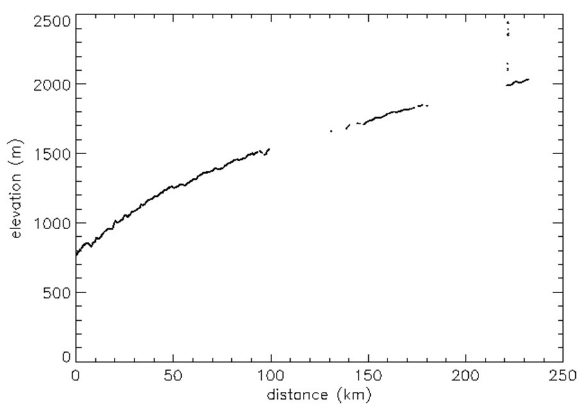

Figure 2. An AOL profile from the Greenland ice sheet.

At a distance of approximately 230 km the AOL can be seen to "lose lock" of the surface, most probably due to the presence of cloud. In Figure 3, the mean slope has been removed from the first section of the profile above to indicate the wavelength and amplitude of undulations along the profile.

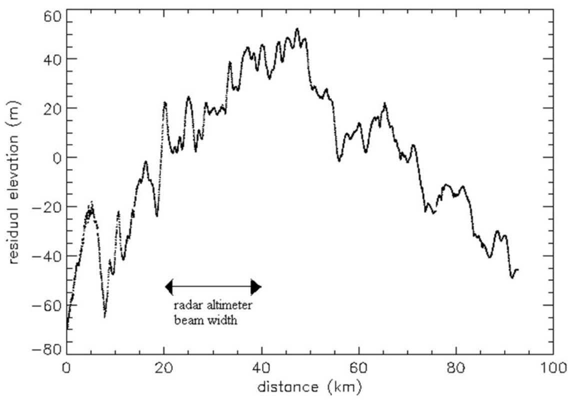

Figure 3. AOL profile for the first 100 km of the track shown in Figure 2, with the mean slope removed.

Undulations with a wavelength of 5-10 km and an amplitude of 15-40 m can be seen, becoming smaller with distance inland (and concurrently, with increasing ice thickness). The approximate width of the RA footprint has been shown to indicate the range of heights which the signal is received from.

2.3 Validation Methodology

The process of relocating the radar altimeter points results in the data no longer lying along a track but instead the points are distributed unevenly, clustered around the peaks of undulations. Combined with the non-regular pattern of AOL flight-lines it was not possible to undertake a conventional cross-over analysis that is usually employed with satellite altimeter data. Instead, all the data were put into a geo-referenced database and the closest AOL point to a given radar altimeter point was identified within the database. Only match-ups within 1 km of each other were included in the results that follow. Four RA points surrounding an AOL point were used to interpolate to the exact location of the AOL point.

3. Results

A shaded planimetric view of the DEM is shown in Figure 4. The shading is a function of elevation and slope, such that higher, flatter regions appear lighter than lower, steeper areas. This highlights the general morphology of the ice sheet but also delineates areas of relative surface roughness such as the drainage basin in the north east, where a long (300 km), linear ice stream has been identified (Fahnestock *et al*, 1993). It can be seen that the flow in much of this basin is affected by the ice stream and that short wavelength undulations "dominate" the local topography, especially south of the ice stream.

Figure 4. A shaded, planimetric view of the 2.5 km resolution DEM of the ice sheet.

32274 points were found where a radar altimeter point lay within 1 km of an AOL value. The complete data set is shown as a function of surface slope (calculated from the DEM) in Figure 5.

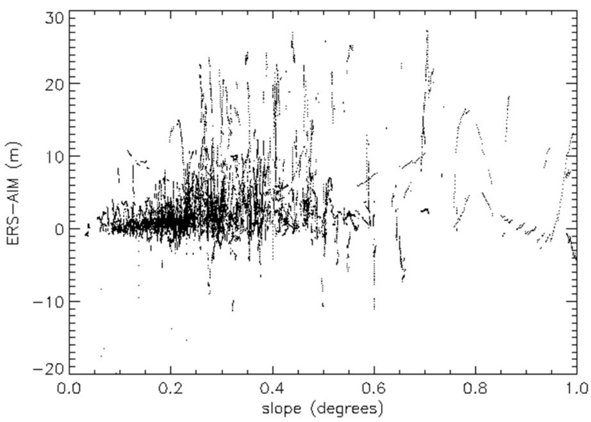

Figure 5. Differences between RA and AOL height estimates lying within 1 km of each other, plotted as a function of surface slope.

There are several features of Figure 5 to note. The half power beam-width of the RA is 0.65° . For regional slopes in excess of this value the accuracy of the RA is likely to be significantly reduced. There are a only a relatively small number of points for slopes greater than this so the predicted degradation is not so apparent, although there is a greater scatter of points above 0.65° . There is a general increase in the spread of points with increasing slope (as would be expected) but this is not as great as previous work has suggested (Figure 7, Ekholm, et al, 1995). There is also a slight increasing positive bias with increasing slope.

These characteristics can also be seen in the tabulated results of the comparison given in Table 1.

slope	**DH (m)**	**s (m)**	**no. points**	**% area**
0-0.1	0.84	0.79	174	2.1
0.1-0.2	1.43	1.95	2557	30.5
0.2-0.3	2.88	3.61	2228	26.6
0.3-0.4	4.37	4.77	1944	23.2
0.4-0.5	7.3	7.03	828	9.8
0.5-0.6	8.36	9.23	287	3.4
0.6-0.7	8.57	8.3	147	1.7
0.7-0.8	10.3	8.4	132	1.5
0.8-0.9	10.07	5.8	80	1.0

Table 1. Statistics for the comparison between the AOL and RA data.

The last column of Table 1 shows the percentage of the ice sheet that has slopes within the range given in column 1. It can be seen that approximately half the ice sheet lies within the slope range 0-0.3° and that the absolute accuracy of the RA data within this range is between 0.84 and 2.9 m. It should be noted that these figures include, not only errors in the RA data, but also errors in the AOL data, which, in principal, should be negligible.

4. Discussion

Table 1 is shown in graphical form in Figure 6.

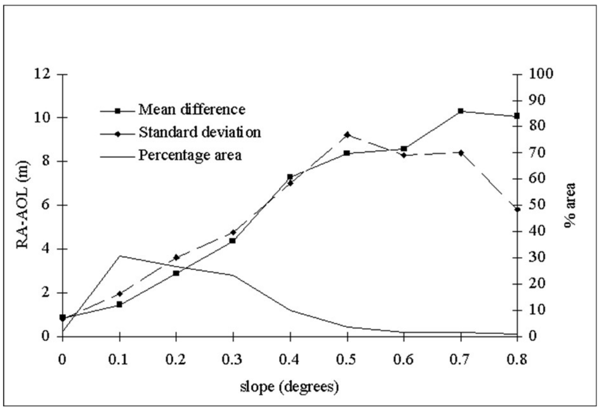

Figure 6. Graphical representation of the data in Table 1: means and standard deviations of the comparison between the AOL and RA data.

As has been observed before (Ekholm *et al,* 1995) the standard deviations increase with increasing slope. Unlike the previous study (which used airborne radar altimeter data for a comparison over Greenland and the direct method for slope correction), the **mean error** is a positive monotonic function of surface slope also. This is due the fact that the relocation method for slope correction places points where they were received from on the surface and this means they are clustered around the peaks of undulations (c.f. Figure 10, Bamber, 1994) whereas the direct method does not do this but introduces much larger random errors (c.f. Table 2, Ekholm *et al*, 1995). This means that only the upper surface of an undulating region is sampled, producing a positive bias (with respect to the mean surface). This effect can be corrected for if an estimate of the average undulation amplitude is known or from using the averaged radar altimeter leading edge width as an estimate of undulation amplitude. Undulation amplitude tends to be governed by ice thickness and bed topography. The former is closely linked to surface elevation and regional slope and it is possible, therefore, to use the results obtained in this study to apply a mean correction to the altimeter data to account for this effect.

A secondary effect is the due to the fact that a single threshold amplitude was used for the waveform retracking. The value used was an optimum one for the whole ice sheet which meant that it will not represent the "true surface" everywhere on the ice sheet. It is suggested that this is the reason for the positive bias for the lowest surface slope regions.

The differences presented in Table 1 and Figure 6 are those for two individual height estimates. When generating the DEM several hundred to thousands of RA points (depending on the latitude) are used to generate an averaged grid point value. The random error in the averaged DEM grid points will be substantially less than that for an individual RA point. To reduce biases in the DEM a linear fit can be applied to the data in Figure 6 and used to correct the grid points as a function of their slope.

It should also be noted that the accuracy of the slope correction procedure is dependent on the across-track spacing and that this is worst for the southern half of the ice sheet. It is expected, therefore, that the results would improve moving northward.

5. Summary

A new 2.5 km DEM of the Greenland ice sheet has been produced from satellite radar altimeter data from the geodetic phase of ERS-1. These data were compared with a high accuracy airborne laser altimeter data set for the southern half of the ice sheet in, what is believed to be, the most complete validation of absolute height determination using satellite radar altimetry over ice. It is hoped to extend this study to include data from the northern half of the ice sheet where, it is expected, the accuracy of the slope correction should be significantly better due to the closer track spacing.

6 Acknowledgements

This work was part funded by a UK NERC grant (GR3/9791) and a British Coucil travel grant to JLB.

7. References

Bamber, J. L. 1994, Ice Sheet Altimeter Processing Scheme. *Int. J. Rem. Sens.*, **14**(4), 925-938.

Bamber, J. L., and P. Huybrechts 1996, Geometric boundary conditions for modelling the velocity filed of the Antarctic ice sheet. *Ann. Glaciol.*, **23**.

Ekholm, S., R. Forsberg, & J.M. Brozena, 1995, Accuracy of satellite altimeter elevations over the Greenland ice sheet. *J. Geophys. Res.* **100** (C2), 2687-2696.

Fahnestock, M.A., R.A. Bindschadler, R. Kwok, and K.C. Jezek 1993, Greenland ice sheet surface properties and ice dynamics from ERS-1 SAR imagery, *Science*, 262, 1530-1534.

Krabill, W.B., R.H. Thomas, C.F. Martin, R.N. Swift, & E.B. Frederick 1995, Accuracy of airborne laser altimetry over the Greenland ice sheet. *Int J. Rem. Sens.* **16** (7), 1211-1222.

Partington, K. C., J. K. Ridley, C.G. Rapley, & H.J. Zwally. 1989, Observations of the surface properties of the ice sheets by satellite radar altimetry. *J. Glaciol.*, **35** (120), 267-275.

Renka, R. L., and A. K. Cline 1984. A triangle-based C interpolation method. *Rocky Mountain J. Math*, **14**, 223-237.